Spherulites of Long-Chain Branched *cis*-1,4-Polybutadiene

Tian-Lai Cheng and An-Chung Su*

Institute of Materials Science and Engineering, National Sun Yat-Sen University, Kaohsiung, Taiwan 80424, Republic of China

Received June 30, 1993; Revised Manuscript Received October 6, 1993•

ABSTRACT: Morphological features of melt crystallized *cis*-1,4-polybutadiene (cPBD) were examined by means of polarized light microscopy. Three samples of similar molecular weight characteristics but different levels of long-chain branching were studied. The two low-branching samples exhibited typical spherulitic morphology. The spherulites were of banded texture at higher crystallization temperatures (T_c); the band period decreased with decreasing T_c and eventually became unidentifiable at T_c < ca. −40 °C. The spherulitic growth rate decreased significantly with the increasing level of branching. The effects of long-chain branching were most dramatically manifested by the surge of small ("dwarf") spherulites in the highly branched cPBD; the dwarf spherulite stopped growing at a size of several microns and induced new dwarf spherulites among its periphery. The process repeated itself to the apparent end of crystallization. The melting temperature of slow-cooled or cold-crystallized samples decreased with the increasing level of branching. These observations were discussed in terms of the entanglement concept.

Introduction

The role of chain entanglement in transport properties of polymer melts is well-known.[1–3] Crystallization of a polymer in its melt state involves transport and rearrangement of entangled chains in the vicinity of the crystal front.[4] Chain entanglement should therefore play a significant role in the melt crystallization of polymers. This was explicitly indicated early in 1963 by Banks et al.[5] in their dilatometric study of bulk crystallization of polyethylene (PE) fractions. With increasing molecular weight, a reversal in the crystallization behavior was identified in the vicinity of M_e where entanglement effects on zero-shear viscosity (η_0) set in. Calvert[6] proposed the formation of loops, with entanglements trapped within, to account for the incomplete crystallization in typical semicrystalline polymers and the apparent Gaussian behavior[7–12] for polymers crystallized under large supercooling. Mansfield et al.[13,14] analyzed the elasticity of entangled chains in the amorphous phase to account for the premelting phenomenon.

In a more recent analysis of polymers crystallized under large supercooling, Robelin-Souffache and Rault[15] observed that the weight-average radius of gyration (R_w) of polymer coils in the melt state controls many solid-state properties such as long period (L), amorphous layer thickness, and crystallinity (χ). In addition, χ varies linearly with R_w^{-1}; an extrapolation to $\chi = 1$ yielded a coil size in accord with M_e. Considering also the identity[7–12] between the radius of gyration of polymer chains in the melt and that in the fast-crystallized solid state, Robelin-Souffache and Rault[15] suggested that, except at small supercooling, entanglements may persist upon crystallization. They proposed further that the competition between crystal growth and chain reptation determines the transition between regimes I and II. A theoretical analysis based on the trapping of entanglements was then provided to explain the observed correlation[15] of $L \sim R_w$ and the well-known variation of L with supercooling.

Disentanglement of chains with long branches is difficult; the reptation time increases exponentially with the branch length.[3] Effects of chain entanglement should therefore be more clearly identifiable in the crystallization of long-chain branched polymers. Earlier investigations of branching effects on crystallization behavior aimed mainly at PE[16–20] (or its copolymers[21–23]) with short branches which act more as defects trapped within (or noncrystallizable species expelled from) the crystal structure[24] than as retarders of chain mobility.

Reported in this article are our preliminary observations on spherulitic features of long-chain branched *cis*-1,4-polybutadiene (cPBD). These cPBD samples are similar in molecular weight but different in the level of long-chain branching. The crystallization and melting behavior of cPBD have been studied on several occasions[25–28] but there appears no report on the corresponding spherulitic morphology.

Table I. Characteristics of cPBD Samples

	B1	B2	B3
M_w[a]	400 000	450 000	430 000
M_n[a]	160 000	170 000	140 000
M_w/M_n[a]	2.5	2.6	3.1
$[\eta]$[b] (dL/g)	2.35	2.28	2.18
$\eta_{5\%}$[c] (mPa·s)	98	80	48
MFI[d] (g/h)	2.20	0.54	0.13
microstructure[e]			
cis configuration (mol %)	96.7	96.6	95.3
trans configuration (mol %)	1.8	1.8	2.5
vinyl configuration (mol %)	1.4	1.5	2.2

[a] Polystyrene-equivalent values from gel permeation chromatography (room temperature, Styrogel columns, differential refractive index detector) using tetrahydrofuran as the carrier solvent. [b] Intrinsic viscosity in toluene at 30 °C. [c] Viscosity of 5 wt % toluene solution at 25 °C, measured by use of a #400 Cannon–Fenske viscometer. [d] Melt flow index determined under a ram load of 3035 g at 100 °C. [e] From infrared spectroscopic analysis.[29]

Experimental Section

Materials. Three cPBD samples, designated as B1, B2, and B3 (in the order of increasing long-chain branching), were synthesized by means of coordination polymerization in benzene using a homogeneous catalyst system of cobalt(II) octanoate and diethylaluminum chloride with the addition of a fixed amount of 1,5-cyclooctadiene (a chain transfer agent to maintain a proper molecular weight level), followed by coagulation and purification in hot water before drying and addition of a minor amount of antioxidant. The extent of long-chain branching was altered by varying the polymerization temperature, which was 40, 50, and 60 °C, respectively, for B1, B2, and B3. These samples were ca. 95–97% *cis* configuration (with ca. 2–3% *trans* and 1–2% vinyl configurations remaining) according to infrared spectroscopic

* To whom correspondence should be addressed.

• Abstract published in *Advance ACS Abstracts*, November 15, 1993.

0024-9297/93/2226-7161$04.00/0

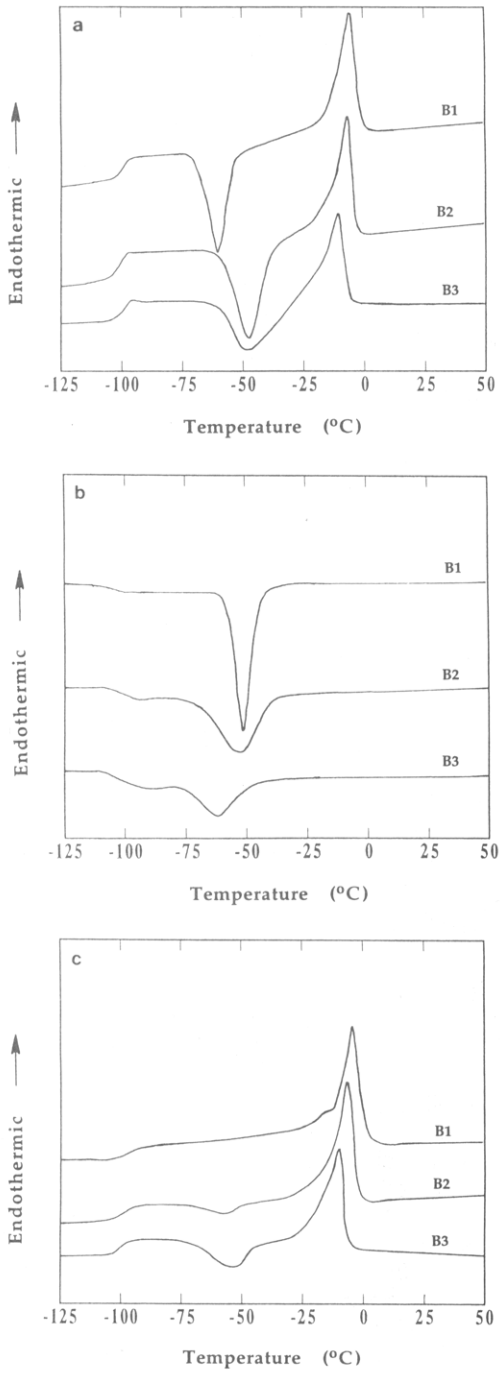

Figure 1. Thermograms of the cPBD samples in (a) the first scan (heating) from the quenched glassy state, (b) the second scan (cooling) from the equilibrated (70 °C) melt, and (c) the third scan (heating) after controlled cooling. Different samples are as marked.

Table II. Summary of Dynamic DSC Scans

sample code	T_{c1} (°C)	T_{m1} (°C)	T_{c2} (°C)	T_{c3} (°C)	T_{m3} (°C)
B1	−59.9	−4.8	−50.2	*a*	−4.6
B2	−46.5	−6.4	−52.3	−56.4	−6.7
B3	−47.1	−10.3	−59.9	−54.1	−10.1

[a] No cold crystallization peak.

analysis.[29] Summarized in Table I are characteristics of these samples determined by means of infrared spectroscopy,[29] gel permeation chromatography (GPC, using tetrahydrofuran as the carrier solvent), solution viscometry (in toluene), and melt flow measurements.

Differential Scanning Calorimetry (DSC). The basic thermal behavior of the cPBD samples was studied by means of differential scanning calorimetry using a Perkin-Elmer DSC7 instrument. The calorimeter was routinely calibrated using an indium standard. Each sample was equilibrated at 70 °C for 3 min and then quickly (ca. −320 °C/min) cooled to −140 °C, followed by three to-and-fro scans between −140 and +70 °C with the rate of heating or cooling fixed at +20 and −20 °C/min.

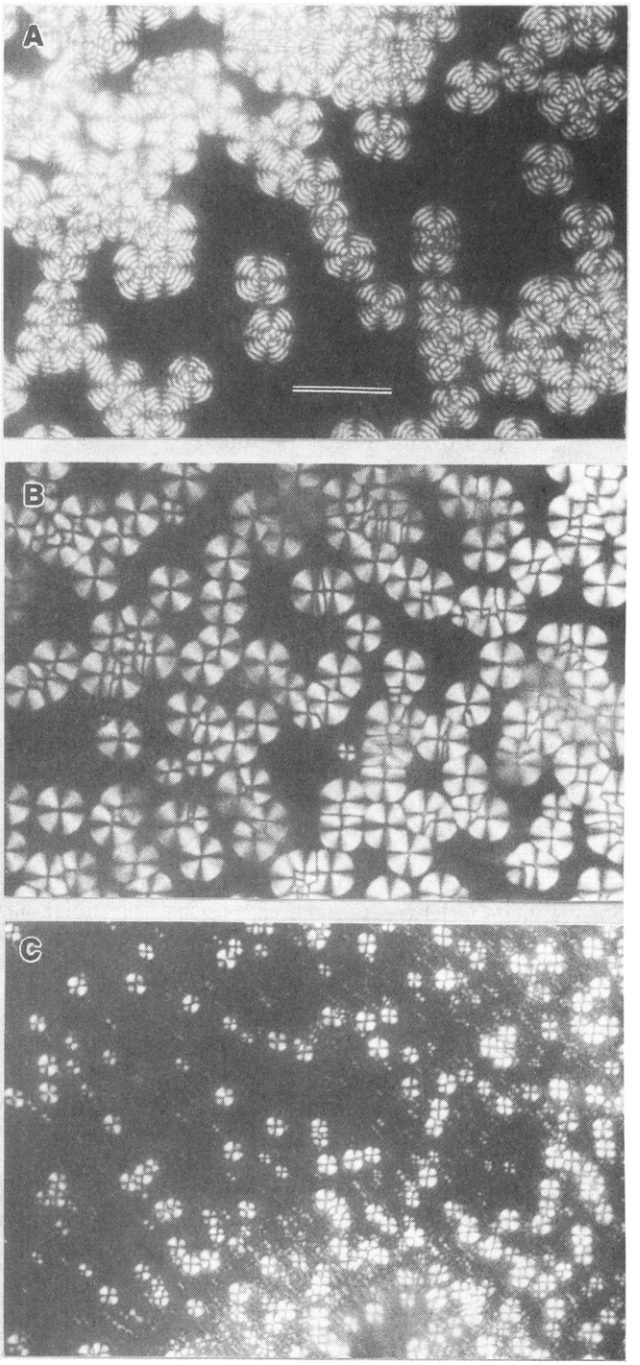

Figure 2. Spherulites formed during isothermal crystallization of B1, observed under cross-polarization after (A) 45 min at −22 °C, (B) 3 min at −40 °C, and (C) 0.7 min at −55 °C. The scale bar corresponds to 50 μm.

Polarized Light Microscopy (PLM). Specimens approximately 20–30 μm in thickness were prepared by casting a drop of the 2% toluene solution on a glass slide, followed by drying under vacuum for 1 h at 100 °C. An optical microscope (Nikon OPTIPHOT-POL) equipped with a Linkam THMS-600 heating stage connected to a TMS-91 temperature controller and a CS-196 liquid-nitrogen cooling system was used. The specimens were heated to an maintained at 70 °C for 3 min, followed by quenching (ca. −150 °C/min) to the respective crystallization temperatures (T_c) where morphological observations were made.

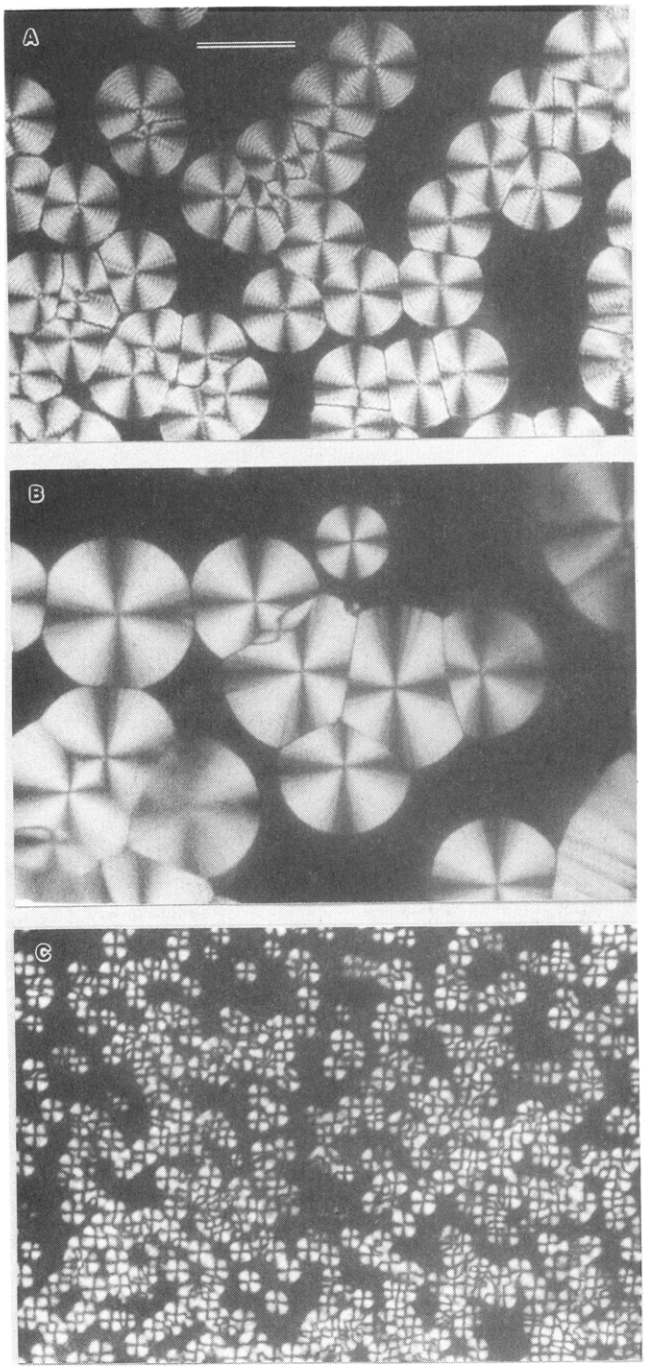

Figure 3. Spherulites formed during isothermal crystallization of B2, observed under cross-polarization after (A) 65 min at −27.5 °C, (B) 16 min at −35 °C, and (C) 1.5 min at −55 °C. The scale bar corresponds to 50 μm.

Results

Sample Characteristics. It may be observed from Table I that dilute solution properties in good solvents (tetrahydrofuran for GPC and toluene in intrinsic viscosity measurements) are similar for the three samples, indicating similar hydrodynamic volumes in the dilute solution state. On the other hand, significant differences exist in the viscosity of concentrated solutions and especially in the melt flow index (MFI) values, indicating significant differences in the level of long-chain branching. Long-chain branching is known to suppress chain dimension in the unperturbed state as compared to the linear counterpart of the same molecular weight; in good solvents (as in the present case of tetrahydrofuran and toluene), however, this effect is partly compensated by the stronger tendency of branched chains to expand.[30] For the present purposes, these samples may therefore be considered similar in molecular weight and polydispersity but significantly different in the level of long-chain branching.

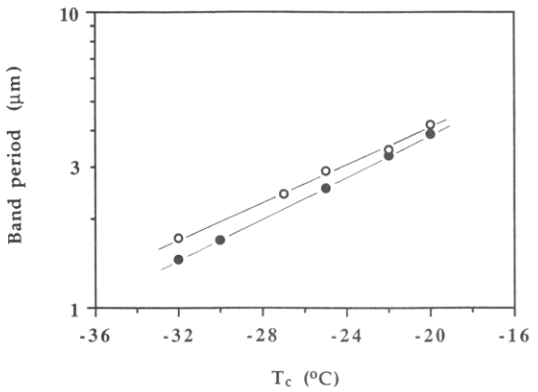

Figure 4. Variation of band period with crystallization temperature for B1 (open symbols) and B2 (filled symbols).

Basic Thermal Behavior. Thermograms of the dynamic DSC scans are shown in Figure 1. Results of the DSC analysis are summarized in Table II. The three samples exhibit essentially the same glass transition temperature (T_g) of ca. −100 °C. In the first heating scan (cf. Figure 1a), an endothermic peak (T_{c1}) corresponding to cold crystallization may be observed above T_g. This is followed by a melting peak (T_{m1}) below 0 °C. It is noted that T_{c1} increases whereas T_{m1} decreases with the level of branching. In the second (cooling) scan (cf. Figure 1b), a single crystallization peak is observed. In this case, the peak temperature of crystallization (T_{c2}) decreases with the increasing level of branching. The crystallization in the high-branching samples is apparently incomplete since a cold crystallization peak (T_{c3}) above T_g may be observed in the following heating scan (cf. Figure 1c). It appears that the low-branching sample crystallizes more readily. The final melting temperature (T_{m3}) also decreases with the increasing level of branching. In fact, values of T_{m1} and T_{m3} are nearly identical for a given sample, in spite of the difference in the crystallization temperature range.

Spherulitic Morphology. Spherulites of B1 and B2, grown during isothermal crystallization, are shown in Figures 2 and 3, respectively. These spherulites are optically negative. For small supercooling (cf. Figures 2A and 3A), banded texture may be observed. The band period decreases with increasing supercooling (Figures 2B and 3B) and becomes unidentifiable for $T_c <$ ca. −40 °C, resulting in small spherulites of radial texture (Figures 2C and 3C). At a given T_c the band period of B1 spherulites is slightly larger than that of the B2 spherulites, as shown in Figure 4.

In the case of the highly branched B3 sample, an unusual type of morphology is manifested. Shown in Figure 5A is the relatively high nucleation density of this sample. The spherulites stop growing (almost immediately after their formation) at a relatively small size of several microns. As may be observed from Figures 5B–D, a "dwarf" spherulite induces new dwarf spherulites along its periphery; the process repeats itself till the apparent end of crystallization.

This peculiar morphology of dwarf spherulites is not limited to the highly branched B3 sample. A closer look at Figure 3C reveals similar (although not as dramatic) features for B2 spherulites under greater supercooling. An approximate morphology map, as shown in Figure 6, may therefore be constructed to represent the effects of the degree of branching and crystallization temperature

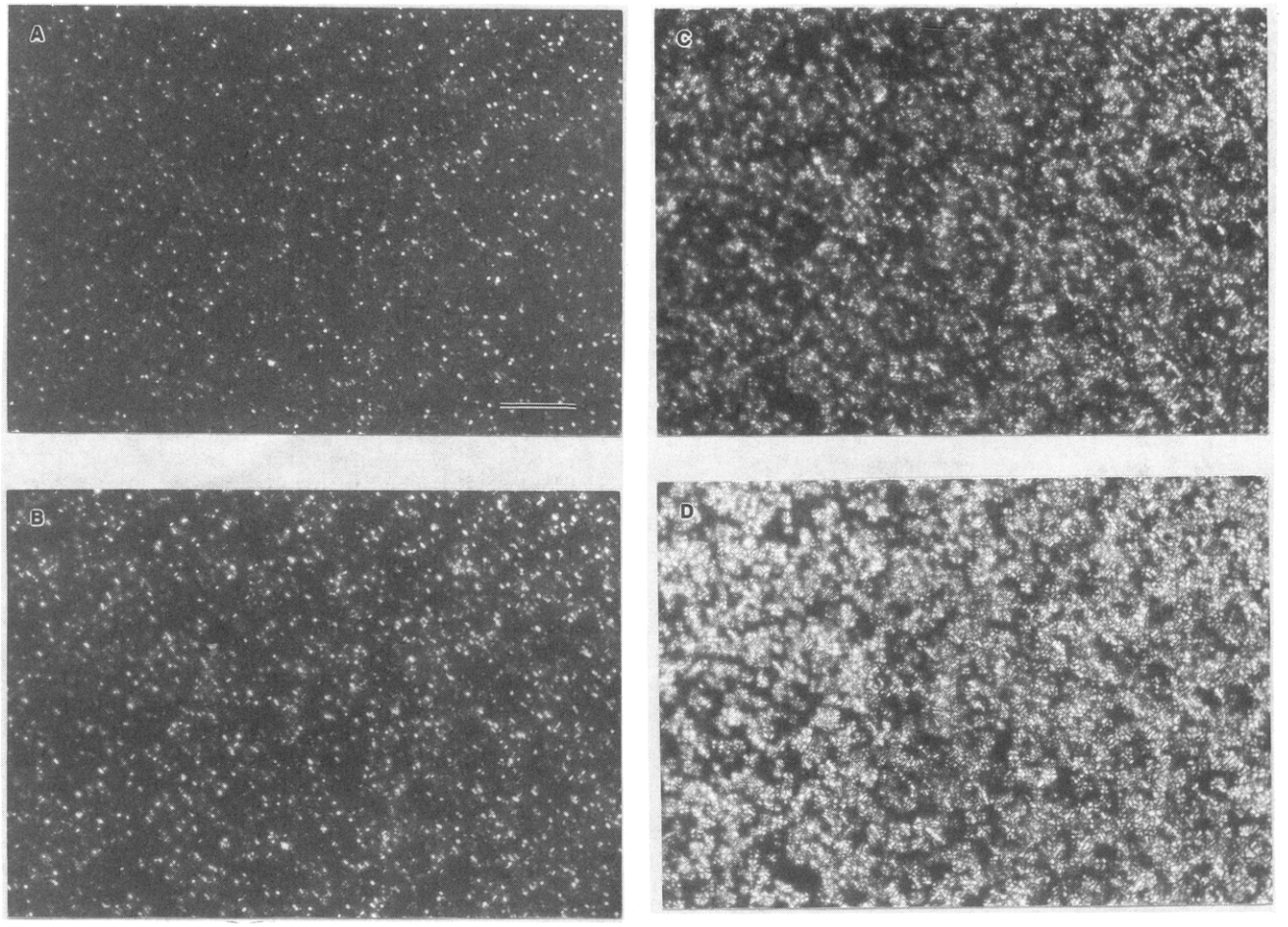

Figure 5. Spherulites formed during isothermal crystallization of B3, observed under cross-polarization after (A) 7.5 min, (B) 9.0 min, (C) 13.5 min, and (D) 16.5 min at −30 °C. The scale bar corresponds to 50 μm.

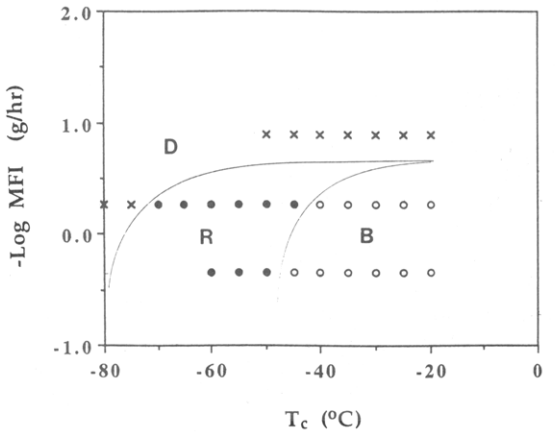

Figure 6. Morphology map for branched cPBD at the present molecular weight level. Crosses, filled circles, open circles correspond to dward, radial, and banded spherulites, respectively. The ordinate represents the relative level of long-chain branching.

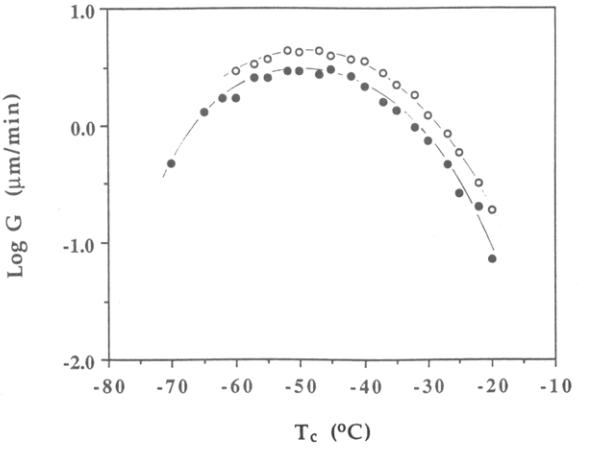

Figure 7. Spherulitic growth rate of B1 (open circles) and B2 (filled circles) at various crystallization temperatures.

on spherulitic morphology of cPBD at the present molecular weight level.

Growth Rate. Due to the peculiar features of dwarf spherulites described above, the spherulitic growth rate (G) of the B3 sample could not be accurately determined. Logarithmic growth rates of B1 and B2 spherulites at various T_c are shown in Figure 7. The cruves are parabolic in shape, with the maximum located in the vicinity of −50 °C. The growth rate decreases with the increasing level of branching. It may also be noted that these curves are approximately parallel, suggesting that the effect of long-chain branching does not vary strongly with crystallization temperature. The earlier observation that B1 is more readily crystallizable during the dynamic DSC scans may therefore be attributed to the corresponding higher growth rate.

Discussion

Spherulitic Texture. Banded spherulites are believed to consist of lamellae twisting[31-35] or curving[36] in concert along the radial direction. The concerted twisting or curving of lamellae has been attributed to the asymmetric stresses set up within disordered folds or the presence of screw dislocations.[37] The present observation indicates dissipation of band texture at the low T_c end (i.e., large

supercooling) via the diminishing band period with increasing growth rate. This is rather similar to the case of polyethylene (PE).[33] It should be noted that the disappearance of bands in PE spherulites may also occur by coarsening of the band texture (and a gradual transition to axialites) with decreasing growth rate at the other extreme of small supercooling.[33] As noted previously,[38] banded spherulites may often be obtained within a moderate range of growth rate, lying typically in the high-temperature branch of the G–T_c curve and being encompassed by the low growth rate region of axialites and the high growth rate region of radial spherulites. Although the behavior of cPBD at the low-supercooling end was not specifically examined in the present study due to the long crystallization time involved, a similar behavior is expected.

It is then interesting to note that, in the case of polyesters such as poly(ε-caprolactone) (PCL) and polyamides, the trend in growth rate dependence of band period is reversed in the presence of a small amount of miscible polymeric diluents which suppress spherulitic growth but induce finely banded textures.[39] This has been attributed to the adsorption of the foreign entities on crystal boundaries.[39] Similar observations have been made for blends of linear PE fractions[40] and blends of PCL and poly(styrene-*co*-acrylonitrile)[41] but at higher diluent levels. It is therefore clear that the macroscopic growth rate is generally not a fundamental factor controlling spherulitic texture, as noted previously.[33] The dynamic competition among splaying, twisting or curving, and branching of lamellae at the crystal front appears more consistent with the present knowledge of spherulitic growth.[42,43]

Growth Rate. The decreasing spherulitic growth rate with increasing branching level is more or less expected. A similar trend has been reported by Lopez et al.[44] for their long-chain branched poly(*p*-phenylene sulfide) (PPS) samples (with M_w = 63 000–75 000) containing 0–0.2 mol % trifunctional branching units. Qualitatively, the decreased growth rate may be attributed to the decreased chain mobility with increasing branching. More specifically, the decrease in chain mobility should reflect an increase in reptation time. By identifying the reptation rate with the folding rate in regimes I and II, Hoffman[45] suggested that the spherulitic growth rate should be inversely proportional to molecular weight in the case of linear polymers. This was in reasonable agreement with previous growth rate data[46] of linear PE fractions in the vicinity of the regime I–II transition, although a later consideration on the free energy change associated with the adsorption of the first stem resulted in a slight modification[47] of the predicted molecular weight dependence. However, observations on other linear polymers such as PPS,[48] poly(ethylene oxide),[49] and poly(aryl ether ether ketone)[50] (PEEK) appeared at variance with this prediction.

As explained by de Gennes,[3] the reptation time of a branched chain increases exponentially with the branch length. This is in agreement with earlier[51] and more recent[52] melt viscosity data of branched polymers. In addition, the MFI values have been shown[53] to vary linearly with η_0^{-1}. As an approximation, therefore, we may take the reciprocal of MFI of the present cPBD samples as a relative measure of reptation time. It follows that the relative reptation times of the present cPBD samples follow the order B1:B2:B3 = 1:4:17. The corresponding ratio between growth rates of B1 and B2 is ca. 1.5 (cf. Figure 7), lower than expected from the proposed dependence of growth rate on reptation time. This may probably be attributed to incomplete disentanglement of the crystallizing chains at the crystal front. On the other hand, the nearly complete suppression of growth in the case of B3 is stronger than that predicted by this direct reptation argument. Additional factors, such as the elasticity force experienced by a crystallizing chain discussed below, must have interfered.

Dwarf Spherulites. This type of morphology is not limited to highly branched chains. As noted earlier, the moderately branched B2 sample also exhibits this feature at a comparatively lower T_c range. Futhermore, in an earlier microscopic study of linear PEEK by Deslandes et al.,[50] spherulites of high molecular weight samples exhibited similar behaviors (cf. their Figure 2). The formation of dwarf spherulites appears related to the suppressed growth rate *and* the stronger tendency of *induced* nucleation. The latter may probably be related to the strain of entangled chains at the crystal front in a manner similar to strain-induced crystallization of cross-linked rubber. As the reptation time increases, the folding of a chain (as driven by the crystallization "force"[14]) attached to the crystal front no longer results in the pull-out of the chain from the melt pool but, instead, deforms the entangled rubbery matrix near the crystal front. The crystallization force is therefore balanced by the rubber elasticity force, resulting in a stronger suppression of growth rate as noted earlier. This strained network at the crystal front may subsequently induce primary nucleation of new spherulites, presumably due to the alignment of stretched chains.

Melting. The decreasing melting temperature (T_{m3}) with the increasing level of branching and the insensitivity of T_{m3} to the crystallization temperature range deserve some comments. These should not be related to the presence of branch points as defects in the crystals; unlike the short-branch case such as low-density polyethylene or linear low-density polyethylene, the long branches in the present cPBD require only a limited number of branch points. These observations may be more suitably attributed to the melting–reorganization–remelting mechanism.[54–59] In terms of this model, chains of higher mobility (i.e., lower level of branching) should be capable of reorganization up to a higher temperature during the DSC scan and therefore should exhibit a higher final melting temperature. Consequently, for a given sample, the difference in lamellar thickness (and therefore the melting temperature) due to the difference in the crystallization temperature range should be smeared by the reorganization process during the DSC scan; the nearly constant value of T_{m3} then simply reflects the high-temperature end of the competing reorganization process at the present heating rate.

On the other hand, microscopic observations[60] on other cPBD samples (of lower molecular weight) do indicate the presence of two types of crystals of separate orientations and melting temperatures, in accordance with the dual-population mechanism proposed more recently.[61–63] This model is consistent with the dual-morphology picture of the spherulitic structure proposed earlier by Basset et al.[64] In terms of the dual-morphology model, we may attribute the final melting peak to the dominant lamellae which, developed first during spherulitic growth, are comparatively thick and melt at higher temperature. The melting temperature of the space-filling, subsidiary lamellae is comparatively low and varies more significantly with T_c. In the present case of steady cooling, the melting of subsidiary lamellae is likely to spread over a relatively wide temperature range. This would explain the apparent absence of the melting endotherm for subsidiary lamellae except in the case of B1 where a shoulder at ca. −20 °C

may be identified in the third scan (Figure 1c) but was absent in the first DSC scan (Figure 1a). This shoulder probably corresponds to thickened subsidiary lamellae due to the annealing effect from the relatively low cooling rate in the preceding DSC scan, as separate observations on melting behavior of isothermal crystallized cPBD appear to indicate.[65] The model would then suggest that lamellar thickness of the dominant lamellae decreases with long-chain branching. This, along with the observation that the (final) melting temperature of the dominant lamellae (and hence T_{m3} here) is insensitive to T_c, would require more involved explanations, as to be discussed in a future report along with more extensive observations on the melting behavior of cPBD. It suffices to state here that neither of the two mechanisms can be confidently eliminated for the present system; in fact, the simplest way to integrate these observations is to assume that both of the two mechanisms can be effective, as similarly indicated in earlier studies of PEEK[63] and PPS.[66]

Conclusions

In summary, we have presented spherulitic features of melt crystallized cPBD with different levels of long-chain branching at different crystallization temperatures. Of particular interest is the observation of "dwarf" spherulites in the highly branched cPBD sample. These dwarf spherulites stopped growing at a size of several microns and induced new dwarf spherulites along its periphery. The process repeated itself to the apparent end of crystallization. In addition, the melting temperature of slow-cooled or cold-crystallized samples decreased with the increasing level of branching. These were discussed in terms of the entanglement concept.

Acknowledgment. Thanks are due to Mr. Chia-Ting Chung at IMSE for his help in the PLM study. This work is financially supported by the National Science Council, ROC, under Contract No. NSC83-0405-E110-015.

References and Notes

(1) Graessley, W. W. *Adv. Polym. Sci.* **1976**, *16*, 1.
(2) Graessley, W. W. *Adv. Polym. Sci.* **1982**, *47*, 67.
(3) de Gennes, P. G. *Scaling Concepts in Polymer Physics*; Cornell University Press: Ithaca, NY, 1979.
(4) Wunderlich, B. *Macromolecular Physics*; Academic: New York, 1976; Vol. 2.
(5) Banks, W.; Gordon, M.; Role, R.-J.; Sharples, A. *Polymer* **1963**, *4*, 41.
(6) Calvert, P. *J. Polym. Sci., Polym. Phys. Ed.* **1979**, *17*, 1341.
(7) Schelten, J.; Ballard, D. G.; Wignall, G. D.; Longman, G.; Schmatz, W. *Polymer* **1976**, *17*, 751.
(8) Guenet, J. M.; Picot, C.; Benoit, H. *Faraday Discuss. Chem. Soc.* **1979**, *68*, 251.
(9) Stamm, M.; Fischer, E. W.; Dettenmaier, M. D. *Faraday Discuss. Chem. Soc.* **1979**, *68*, 263.
(10) Ballard, D. E.; Burgess, A. N.; Crowley, T. L.; Longman, G. W. *Faraday Discuss. Chem. Soc.* **1979**, *68*, 279.
(11) Yoon, D. Y.; Flory, P. J. *Faraday Discuss. Chem. Soc.* **1979**, *68*, 388.
(12) Wignall, G. D.; Mandelkern, L.; Edwards, C.; Glotin, M. *J. Polym. Sci., Polym. Phys. Ed.* **1982**, *20*, 245.
(13) Mansfield, M. L. *Macromolecules* **1987**, *20*, 1384.
(14) Rieger, J.; Mansfield, M. L. *Macromolecules* **1989**, *23*, 8310.
(15) Robelin-Souffache, E.; Rault, J. *Macromolecules* **1989**, *22*, 3581.
(16) Mandelkern, L.; Maxfield, J. *J. Polym. Sci., Polym. Phys. Ed.* **1979**, *17*, 1913.
(17) Strobl, G. R.; Schneider, M. J.; Voigt-Martin, I. G. *J. Polym. Sci., Polym. Phys. Ed.* **1980**, *18*, 1361.
(18) Mandelkern, L.; Glotin, M.; Benson, R. A. *Macromolecules* **1981**, *14*, 22.
(19) Glotin, M.; Mandelkern, L. *Macromolecules* **1981**, *14*, 1394.
(20) Maderek, E.; Strobl, G. R. *Colloid Polym. Sci.* **1983**, *261*, 471.
(21) Voigt-Martin, I. G.; Alamo, R.; Mandelkern, L. *J. Polym. Sci., Polym. Phys. Ed.* **1986**, *24*, 1283.
(22) Alamo, R. G.; Mandelkern, L. *Macromolecules* **1991**, *24*, 6480.
(23) Alamo, R. G.; Chan, E. K. M.; Mandelkern, L.; Voigt-Martin, I. G. *Macromolecules* **1992**, *25*, 6381.
(24) Hay, J. N.; Zhou, X.-Q. *Polymer* **1993**, *34*, 1002.
(25) Mitchell, C. J. *J. Polym. Sci., Polym. Lett.* **1963**, *1*, 285.
(26) Collins, E. A.; Chandler, L. A. *Rubber Chem. Technol.* **1966**, *39*, 193.
(27) Mitchell, J. C. *Polymer* **1967**, *8*, 369.
(28) De Chirico, A.; Lanzani, P. C.; Raggi, E.; Bruzzone, M. *Makromol. Chem.* **1974**, *175*, 2029.
(29) Silas, R. S.; Yates, J.; Thornton, V. *Anal. Chem.* **1959**, *31*, 529.
(30) Berry, G. C.; Hobbs, L. M.; Long, V. C. *Polymer* **1964**, *5*, 31.
(31) Keller, A. *J. Polym. Sci.* **1955**, *17*, 291.
(32) Keller, A.; Wills, H. H. *J. Polym. Sci.* **1959**, *39*, 151.
(33) Keith, H. D.; Padden, F. J., Jr. *Polymer* **1984**, *25*, 28.
(34) Lustiger, A.; Lotz, B.; Duff, T. S. *J. Polym. Sci., Polym. Phys. Ed.* **1989**, *27*, 561.
(35) Keith, H. D.; Padden, F. J., Jr. *J. Polym. Sci., Polym. Phys. Ed.* **1987**, *25*, 2371.
(36) Basset, D. C.; Hodge, H. D. *Polymer* **1978**, *19*, 469.
(37) Basset, D. C. In *Morphology of Polymers*; Sedlacek, B., Ed.; de Gruyter: New York, 1986; p 47.
(38) Li, W.; Yan, R.; Jiang, B. *Polymer* **1992**, *33*, 889 and references cited therein.
(39) Keith, H. D.; Padden, F. J., Jr.; Russell, T. P. *Macromolecules* **1989**, *22*, 666.
(40) Lopez, J. M. R.; Gedde, U. W. *Polymer* **1988**, *29*, 1037.
(41) Li, W.; Yan, R.; Jiang, B. *Polymer* **1992**, *33*, 889.
(42) Keith, H. D.; Padden, F. J., Jr. *Polymer* **1986**, *27*, 1463.
(43) Bassett, D. C.; Vaughan, A. S. *Polymer* **1986**, *27*, 1472.
(44) Lopez, L. C.; Wilkes, G. L.; Geibel, J. F. *Polymer* **1989**, *30*, 147.
(45) Hoffman, J. D. *Polymer* **1982**, *23*, 656.
(46) Hoffman, J. D.; Frolen, L. J.; Ross, G. S.; Lauritzen, J. I., Jr. *J. Res. Natl. Bur. Stand., Sect. A* **1975**, *79*, 671.
(47) Hoffmann, J. D.; Miller, R. L. *Macromolecules* **1988**, *21*, 3038.
(48) Lopez, C. L.; Wilkes, G. L. *Polymer* **1988**, *29*, 106.
(49) Cheng, S. Z. D.; Chen, J.; Janimak, J. J. *Polymer* **1990**, *31*, 1018.
(50) Deslandes, Y.; Sabir, F.-N.; Roovers, J. *Polymer* **1991**, *32*, 1267.
(51) Long, V. C.; Berry, G. C.; Hobbs, L. M. *Polymer* **1964**, *5*, 517.
(52) Fetters, L. J.; Kiss, A. D.; Pearson, D. S.; Quack, G. F.; Vitus, F. J. *Macromolecules* **1993**, *26*, 647 and references cited therein.
(53) van Krevelen, D. W. *Properties of Polymers*; Elsevier: Amsterdam, 1976; Chapter 24 and references cited therein.
(54) Wunderlich, B. *Macromolecular Physics*; Academic: New York, 1980; Vol. 3.
(55) Rim, P. B.; Runt, J. P. *Macromolecules* **1983**, *16*, 762.
(56) Blundell, D. J.; Osborn, B. N. *Polymer* **1983**, *24*, 953.
(57) Lee, Y.; Porter, R. S. *Macromolecules* **1987**, *20*, 1336.
(58) Blundell, D. J. *Polymer* **1987**, *28*, 2248.
(59) Nichols, M. E.; Robertson, R. E. *J. Polym. Sci., Polym. Phys. Ed.* **1992**, *30*, 305.
(60) Cheng, T. L.; Su, A. C. Manuscript in preparation.
(61) Cheng, S. Z. D.; Cao, M.-Y.; Wunderlich, B. *Macromolecules* **1986**, *19*, 1868.
(62) Cebe, P.; Hong, S.-D. *Polymer* **1986**, *27*, 1183.
(63) Basset, D. C.; Olley, R. H.; Al Raheil, I. A. M. *Polymer* **1988**, *29*, 1745.
(64) Basset, D. C.; Hodge, A. M. *Proc. R. Soc. London* **1981**, *A377*, 25, 39, 61.
(65) Cheng, T. L.; Su. A. C. Unpublished results.
(66) Chung, J. S.; Cebe, P. *Polymer* **1992**, *33*, 2312.